=Electronic Supplementary Information=

# Supramolecular linear coordination polymers of human serum albumin and haemoglobin

Ryo Adachi, Shun Suzuki, Tatsuya Mitsuda, Yoshitsugu Morita, and Teruyuki Komatsu*

Department of Applied Chemistry, Faculty of Science and Engineering, Chuo University, 1-13-27 Kasuga, Bunkyo-ku, Tokyo 112-8551, Japan

Corresponding author: Prof. Teruyuki Komatsu

Tel & Fax: +81-3-3817-1910, E-mail: komatsu@kc.chuo-u.ac.jp

## Experimental section

### Materials and mehods

4’-Chloro-2,2’:6’,2”-terpyridine, 2-aminoethanol, and *N*-succinimidyl 4-(*N*-maleimidomethyl)cyclohexanecarboxylate were purchased from Fujifilm Wako Pure Chemical Corp. Human serum albumin (HSA, Albumin 25%-Benesis) was purchased from the Japan Blood Products Organization. Pure human adult hemoglobin was purified from red blood cell concentrate received from the Japanese Red Cross Society. All other reagents and solvents were of commercial high-purity grades and were used without further purification. Deionized water (18.2 MΩ·cm) was prepared using water purification systems (Elix UV and Milli-Q Reference; Millipore Corp.). The UV-vis absorption spectra were recorded using a UV-visible spectrophotometer (8543; Agilent Technologies Inc.) connected with a temperature control unit (89090A; Agilent Technologies Inc.). Circulation dichroism (CD) spectra were obtained using a CD spectrometer (J-820; Jasco Corp.) at 25°C. Mass spectra were mesured using a MALDI-TOF mass spectrometer (AXIMA-CFR; Shimadzu Corp.) or an ESI-TOF mass spectrometer (JMS-T100CS; JEOL Ltd.). Thin-layer chromatography (TLC) was carried out on 0.2 mm precoated plates of silica gel 60 $F_{254}$ (Merck KGaA). The $^1$H-NMR spectra were recorded using an FT NMR spectrometer (ECA 500; JEOL Ltd.). The chemical shift of the $^1$H-NMR spectrum was referenced to the residual $CHCl_3$ solvent signal. Dynamic light scattering (DLS) measurements were performed using a zeta-potential and particle size analyser (ELSZ-2000ZS; Otsuka Electronics Co., Ltd.).

**4’-(2’’’-Aminoethoxy)-2,2’:6’,2”-terpyridine ($NH_2$-Tpy)**

KOH (200 mg, 3.56 mmol) was grounded in an agate mortar and was dispersed in DMSO (4.0 mL). 4’-Chloro-2,2’:6’,2”-terpyridine (114 mg, 0.43 mmol) and 2-aminoethanol (60 μL, 0.99 mmol) were added to the KOH dispersion in DMSO and the mixture was stirred for 5 h at 50°C in the dark. After removing the solvent by freeze-drying, the residue was dissolved in $CH_2Cl_2$. The organic layer was washed three times with water and dried over anhydrous $Na_2SO_4$. The solution was evaporated to give a pale-yellow solid, $NH_2$-Tpy (79 mg). $R_f$ = 0.24 ($CHCl_3$/$CH_3OH$ = 10/1, v/v), Yield 63%. $^1$H-NMR ($CDCl_3$) $\delta$: 8.61 (d, 2H, pyridyl-2’), 8.53 (d, 2H, pyridyl-3’), 7.96 (s, 2H, pyridyl-3), 7.78 (t, 2H, pyridyl-4’), 7.25 (t, 2H, pyridyl-3’), 4.19 (t, 2H, ethoxy-1’’’), 3.07 (t, 2H, ethoxy-2’’’). ESI-MS (*m/z*) calcd. For $C_{17}H_{16}N_4O$, 292.34; found 292.9 $[M]^+$.

**4’-{2’’’-[4””-(*N*-Maleimidomethyl)cyclohexanoylamino]ethoxy}-2,2’:6’,2”-terpyridine (1)**

*N*-Succinimidyl 4-(*N*-maleimidomethyl)cyclohexanecarboxylate (10.6 mg, 31.7 mmol) was added into a DMSO solution (9.35 mL) of $NH_2$-Tpy (13.9 mg, 47.5 mmol), and the mixture was stirred for 18 h at 25°C in the dark. After removing the solvent by freeze-drying, the residue was dissolved in $CHCl_3$ and was chromatographed on aluminum oxide 60 (Merck KGaA) using $CHCl_3$/ethanol = 200/1 (v/v) as the eluent. The solution of the collected band was evaporated to give a white solid **1** (11.7 mg). $R_f$ =

0.33 ($CHCl_3$/$CH_3OH$ = 200/1, v/v), Yield 72%. $^1$H-NMR ($CDCl_3$) $\delta$: 8.62 (d, 2H, pyridyl-2'), 8.54 (d, 2H, pyridyl-3'), 7.95 (s, 2H, pyridyl-3), 7.79 (t, 2H, pyridyl-4'), 7.27 (m, 2H, pyridyl-3'), 6.61 (s, 2H, maleimide), 5.90 (s, 1H, amide), 4.23 (t, 2H, ethoxy-1'''), 3.66 (t, 2H, ethoxy-2'''), 3.29 (d, 2H, maleimide-$CH_2$-), 1.98 (m, 1H, cyclohexane-1''''), 1.84 (d, 2H, cyclohexane-2''''), 1.67 (m, 3H, cyclohexane-2'''',4''''), 1.38 (q, 2H, cyclohexane-3''''), 0.93 (q, 2H, cyclohexane-3''''). ESI-MS (*m/z*) calcd. For $C_{29}H_{29}N_5O_4$, 511.57; found 512.4 $[M]^+$, 534.4 $[M+Na]^+$.

**Expression of HSA(K378C)**

The HSA(K378C) mutant was prepared according to our previously reported procedure.[8] The mutation (K378C) was introduced into the HSA coding region in a plasmid vector encoding the HSA using a QuikChange II site-directed mutagenesis kit (Agilent Technologies Inc.). The mutation was confirmed by DNA sequencing. The plasmid was then digested by *Sal*I and introduced into yeast (*Pichia pastoris* GS115) by electroporation using an Electroporator (MicroPulser; Bio-Rad Laboratories, Inc.). The expression protocol and purification method were described earlier.[8] Briefly, the clones were grown in a buffered glycerol-complex (BMGY) medium in a shaking incubator (Bio-Shaker G·BR-200; Taitec Corp.) at 30°C (250 rpm). Subsequently, the growth cell was resuspended in a buffered methanol-complex (BMMY) medium. To induce expression, the suspension was continued to shake in the incubator at 30°C (300 rpm) for 10 days. During the cultivation, methanol (1% volume of medium) was added every 24 h.

The obtained protein was harvested from the supernatant of the growth medium by precipitation with ammonium sulfate and purified by a Cibacron Blue column with a Blue Sepharose 6 Fast Flow (GE Healthcare UK Ltd.). The HSA(K378C) was finally subjected to gel filtration chromatography (GFC) with a Sephadex G-25 Superfine (GE Healthcare UK Ltd.) using 50 mM phosphate buffer (PB) solution (pH 7.0). The protein concentration was ascertained using a Pierce 660nm Protein Assay Kit (Thermo Fischer Scientific, Inc.).

**Expression of Hb(βC93A/βK120C)**

The Hb(βC93A/βK120C) mutant was prepared according to our previously reported procedure.[12] The second mutation (βC93A) was introduced into the HSA coding region in a plasmid vector encoding the HSA(βK120C) mutant using a QuikChange II site-directed mutagenesis kit. The mutation was confirmed by DNA sequencing. The plasmid was digested by *Sal*I and introduced into yeast (*Pichia pastoris* GS115) by electroporation. The expression protocol and purification method were as previously described.[12] Briefly, the clones were grown in a BMGY medium at 30°C (180 rpm) and transferred to a BMMY medium containing 0.3 mM hemin for induction with methanol in a shaking incubator at 30°C (200 rpm) for 6 days. The induced medium was centrifuged and washed with 20 mM PB (pH 6.0) containing 1 mM phenylmethylsulfonyl fluoride. Then, the cells were disrupted using a homogenizer (BeadBeater; BioSpec Products Inc.) with glass beads. After centrifugation (12,000 × *g*,

1 h), the obtained supernatant was flowed CO gas to avoid the heme oxidation. The lysate was subjected to cation exchange chromatography (CEC) with a SP Sepharose Fast Flow (GE Healthcare UK Ltd.). After washing out unnecessary proteins, Hb(βC93A/βK120C) was eluted. Thereafter, the eluent was loaded onto anion exchange chromatography (AEC) with a Q Sepharose Fast Flow (GE Healthcare UK Ltd.). Finally, the Hb(βC93A/βK120C) was eluted using 20 mM Tris-HCl solution (pH 8.0).

**HSA($Tpy_2$)**

To reduce the partially oxidized Cys-34 and Cys-378 residues of HSA(K378C), the PB solution (50 mM, pH 7.0) of dithiothreitol (DTT, 20 mM, 320 μL) was added to the PB solution of HSA(K378C) (100 μM, 8 mL) under $N_2$ atmosphere. The mixture was stirred for 1.75 h under $N_2$ atmosphere at 25°C in the dark. Excess DTT was removed using GFC with a Sephadex G-25 superfine (GE Healthcare UK Ltd.). The percentage of the reduced form of Cys (mercapto rate) was ascertained using 4,4'-dithiopyridine (4DTP)[9] as 191%. This result indicates that both Cys residues of HSA(K378C) are in the reduced form.

Subsequently, DMSO solution of **1** (267 μM, 10.5 mL) was slowly added dropwise into the PB solution (50 mM, pH 7.0) of HSA(K378C) (10 μM, 70 mL), and the reaction mixture was stirred for 24 h at 25°C in the dark. The solution volume was reduced to 10 mL using a centrifugal concentration device (Vivaspin, 10 kDa MWCO; Sartorius AG) at 4°C. After filtration using a syringe filter unit (Millex-GP 0.22 μm; Merck KGaK), unreacted **1** was removed by GFC with a Sephadex G-25 superfine using 50 mM PB (pH 7.0). The obtained HSA($Tpy_2$) solution was concentrated using a Vivaspin to 10 mL.

Aqueous EDTA solution (100 mM, 1 mL) was added to the obtained HSA($Tpy_2$) solution, and the mixture was stirred for 18 h at 25°C in the dark. To remove excess EDTA properly, the reaction mixture was subjected to GFC with a Sephadex G-25 superfine using deionized water, and the eluent was further washed by concentration and dilution cycles using Vivaspin with deionized water. This washing cycle was repeated over 10 times. The mercapto rate was ascertained as 3%, indicating that the two maleimide groups were introduced into the HSA(K378C). The yield was 60%.

**Hb($Tpy_2$)**

The Hb($Tpy_2$) was synthesized according to the same procedure described above. DMSO solution of **1** (1.07 mM, 0.6 mL) was slowly added dropwise into the phosphate-buffered saline (PBS) solution of Hb(βC93A/βK120C) (CO complex, 20 μM, 4 mL), and the reaction mixture was stirred for 24 h at 25°C under CO atmosphere in the dark. After filtration using a syringe filter unit (Millex-GP 0.22 μm), the unreacted **1** was removed by GFC with a Sephadex G-25 superfine using 50 mM PB (pH 7.0). The obtained Hb($Tpy_2$) solution was concentrated using Vivaspin to 5 mL.

Aqueous EDTA solution (100 mM, 0.1 mL) was added to the obtained Hb($Tpy_2$) solution, and the mixture was stirred for 18 h at 25°C in the dark. To remove excess EDTA properly, the reaction mixture

was subjected to GFC with a Sephadex G-25 superfine using deionized water, and the eluent was further washed by concentration and dilution cycles using Vivaspin with deionized water. The mercapto rate was ascertained as 8%, representing that the two maleimide groups were introduced into the molecule. The yield was 73%.

**[HSA(Tpy$_2$)–Fe$^{2+}$]$_n$ nanofibres and [Hb(Tpy$_2$)–Fe$^{2+}$]$_n$ nanofibres**

**(i) Molar ratio method.** The 10 μL of aqueous solution of $FeCl_2$ (440 μM freshly prepared) was injected to the HSA(Tpy$_2$) solution in deionized water (22 μM, 2.0 mL) ([$FeCl_2$]/[HSA(Tpy$_2$)] = 0.1, mol/mol) and UV-vis absorption spectrum was measured after 30 min. This operation was repeated until the [$FeCl_2$]/[HSA(Tpy$_2$)] reaches 1.5 (mol/mol). Moreover, the UV-vis absorption spectra were measured at [$FeCl_2$]/[HSA(Tpy$_2$)] = 2.0, 2.5, and 3.0 (mol/mol).

Similarly, 5.0 μL of aqueous solution of $FeCl_2$ (165 μM freshly prepared) was injected into the Hb(Tpy$_2$) solution in deionized water (CO complex, 5.5 μM, 1.5 mL) ([$FeCl_2$]/[Hb(Tpy$_2$)] = 0.1, mol/mol) and UV-vis absorption spectrum was measured after 30 min. This operation was repeated until the [$FeCl_2$]/[HSA(Tpy$_2$)] reaches 2.0 (mol/mol).

**(ii) Continuous change method.** Each sample solution (450 μL) was prepared by mixing the aqueous $FeCl_2$ solution and HSA(Tpy$_2$) solution (CO complex) with an appropriate ratio; total concentration of $FeCl_2$ and HSA(Tpy$_2$) was 10 μM, and [HSA(Tpy$_2$)]/([HSA(Tpy$_2$)]+[$FeCl_2$]) ranged 0.1, 0.2, 0.3, … 0.9, 1.0). The Job's plots were then prepared using the increase of absorbance (ΔAbs.) at 557 nm.

**(iii) Other measurements, such as structure analysis, enzyme reaction, and $O_2$ binding ability.** Aqueous solution of $FeCl_2$ (200 μM, 0.1 mL) was injected into the aqueous solution HSA(Tpy$_2$) (10 μM, 2.0 mL) or Hb(Tpy$_2$) (10 μM, 2.0 mL) and the mixture was incubated for 6 h to produce the nanofibres.

**[HSA(Tpy$_2$)–Fe$^{2+}$]$_n$ nanotubes and [Hb(Tpy$_2$)–Fe$^{2+}$]$_n$ nanotubes**

The aqueous solution of the [HSA(Tpy$_2$)–Fe$^{2+}$]$_n$ nanofibres (10 μM, 200 μL) in a cryotube was plunged into a liquid nitrogen bath and freeze-dried under a vacuum using a freeze dryer (FDU-1200; Tokyo Rikakikai Co., Ltd.). The [Hb(Tpy$_2$)–Fe$^{2+}$]$_n$ nanotubes were also prepared by the same procedure.

**Cross-linking of [HSA(Tpy$_2$)–Fe$^{2+}$]$_n$ nanotubes and [Hb(Tpy$_2$)–Fe$^{2+}$]$_n$ nanotubes**

1,4-Dixan solution of glutaraldehyde (0.5%, 1.0 mL) was added to the lyophilized [HSA(Tpy$_2$)–Fe$^{2+}$]$_n$ nanotube powder in a cryotube. After 2 min, the supernatant (0.9 mL) was pipetted out and deionized water (0.9 mL) was added to dissolve the unreacted [HSA(Tpy$_2$)–Fe$^{2+}$]$_n$. The concentration of the unreacted [HSA(Tpy$_2$)–Fe$^{2+}$]$_n$ was determined by the UV-vis absorption spectral measurements of the aqueous supernatant. The solvent was changed to deionized water, and the obtained cross-linked nanotubes were dispersed homogeneously using ultra sonication. The cross-linked [Hb(Tpy$_2$)–Fe$^{2+}$]$_n$ nanotubes were also prepared by the same procedure.

**Transmission electron microscopy (TEM)**

The aqueous solution of the [HSA($Tpy_2$)–$Fe^{2+}$]$_n$ nanofibres (3 μL) was placed onto an elastic carbon-coated copper grid (100 mesh; Okenshoji Co. Ltd.). The specimens were stained by 1% sodium phosphotungstate and observed using a transmission electron microscope (HT7700; Hitachi High-Tech Corp.) with accelerating voltage of 100 kV. TEM measurements of the [Hb($Tpy_2$)–$Fe^{2+}$]$_n$ nanofibres were also conducted by the same procedure with 0.2% uranylacetate staining.

**Scanning electron microscopy (SEM)**

The lyophilized sample of the [HSA($Tpy_2$)–$Fe^{2+}$]$_n$ nanotubes or [Hb($Tpy_2$)–$Fe^{2+}$]$_n$ nanotubes was fixed directly on the carbon tape and sputter-coated with Pd/Pt using an ion sputter (MC1000; Hitachi High-Tech Corp.). The SEM observations were performed using a scanning electron microscope (S-4300; Hitachi High-Tech Corp.) with an accelerating voltage of 10 kV. For each sample, at least 120 different nanotubes were measured to obtain an average size of the outer-diameter. To observe the morphology of the cross-linked nanotubes, the aqueous dispersion of the nanotubes (10 μL) was placed onto a MAS coat slide glass and dried in air for 18 h at 25°C.

**Esterase activity assays**

First, we evaluated an esterase activity of HSA(K378C) in PBS solution (pH 7.4) at 22°C. Several microliters of ethanol solution of *p*-nitrophenylacetate (PNPA) were added to the PBS solution of HSA (4 μM, 2.0 mL) in a 10-mm path length optical quartz cuvette ([PNPA] = 10−100 μM). Immediately after the injection, increases in the absorbance at 405 nm based on the hydrolysed product, *p*-nitrophenol (PNP), were monitored for 10 min. By converting the absorbance increase to the concentration change using a molecular coefficient of PNP [$\varepsilon_{405} = 1.34 \times 10^4$ $M^{-1}$ $cm^{-1}$ in PBS (pH 7.4)],[15] we determined the initial rate constant ($V_0$) for PNPA hydrolysis. The $K_m$ and $k_{cat}$ of PNPA were obtained from Lineweaver–Burk plots using non-linear least squares method.

Second, the esterase activity of the [HSA($Tpy_2$)–$Fe^{2+}$]$_n$ nanofibres was measured. Several microliters of the ethanol solution of PNPA were added to the PBS solution of [HSA($Tpy_2$)–$Fe^{2+}$]$_n$ nanofibres ([HSA($Tpy_2$) unit] = 4 μM, 2.0 mL) in a 10-mm path length optical quartz cuvette ([PNPA] = 10−100 μM) and the $V_0$ was obtained from the absorption change at 405 nm using the procedure described above. The $K_m$ and $k_{cat}$ of PNPA were obtained from Lineweaver–Burk plots using non-linear least squares method.

The esterase activity of the [HSA($Tpy_2$)–$Fe^{2+}$]$_n$ nanotube was measured by the same procedure. Since the dispersion showed strong turbidity, the concentration of HSA($Tpy_2$) unit was reduced to 0.8 μM.

**$O_2$-binding property**

The visible absorption spectral measurements of deoxy (under $N_2$), oxy (under $O_2$), and carbonyl (under CO) forms of the $[Hb(Tpy_2)–Fe^{2+}]_n$ nanofibres ([$Hb(Tpy_2)$ unit] = 10 μM) in PBS (pH 7.4) were carried out with our earlier reported procedures.[12] The $O_2$ affinity ($P_{50}$: $O_2$ pressure where Hb is half-saturated with $O_2$) and Hill coefficient ($n$) were determined using an automatic recording system for the $O_2$ equilibrium curve (Hemox-Analyzer; TCS Scientific Corp.) in PBS (pH 7.4) at 37°C.

## Results

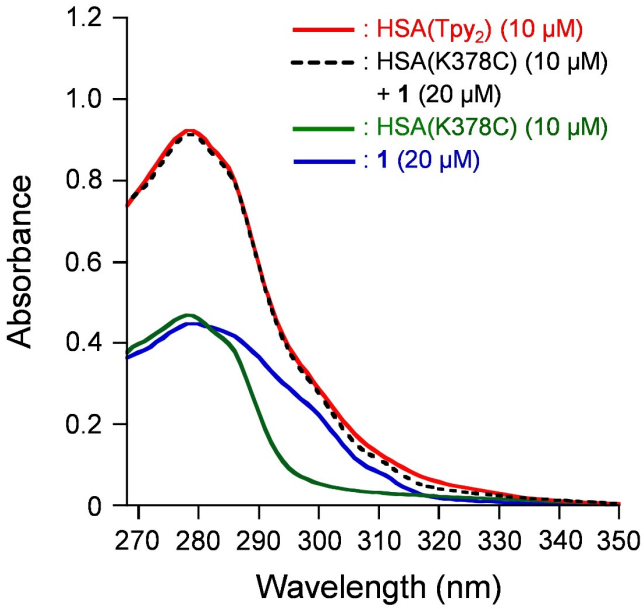


**Fig. S1** UV-vis absorption spectra of HSA(Tpy$_2$) in water (10 μM), HSA(K378C) in PB (10 μM), and maleimide-terpyridine (**1**) in DMSO (20 μM) at 25°C.

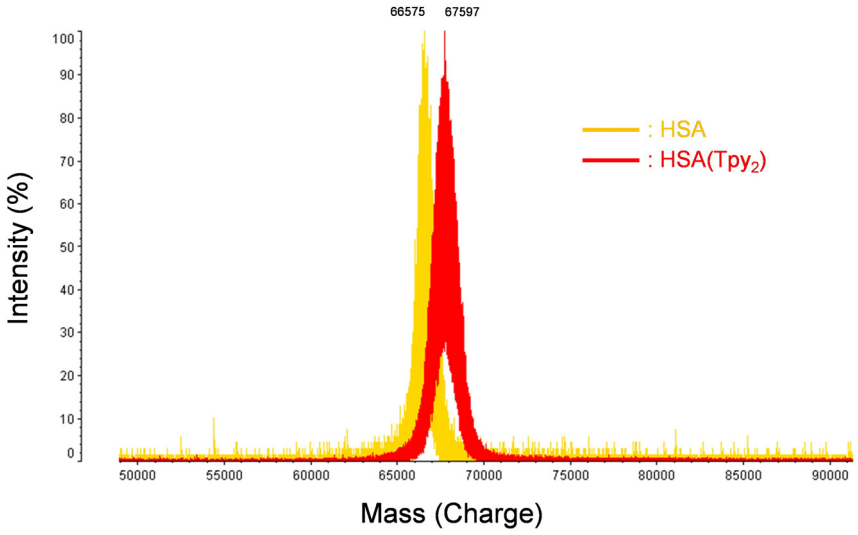


**Fig. S2** MALDI-TOF mass spectra of HSA and HSA(Tpy$_2$).

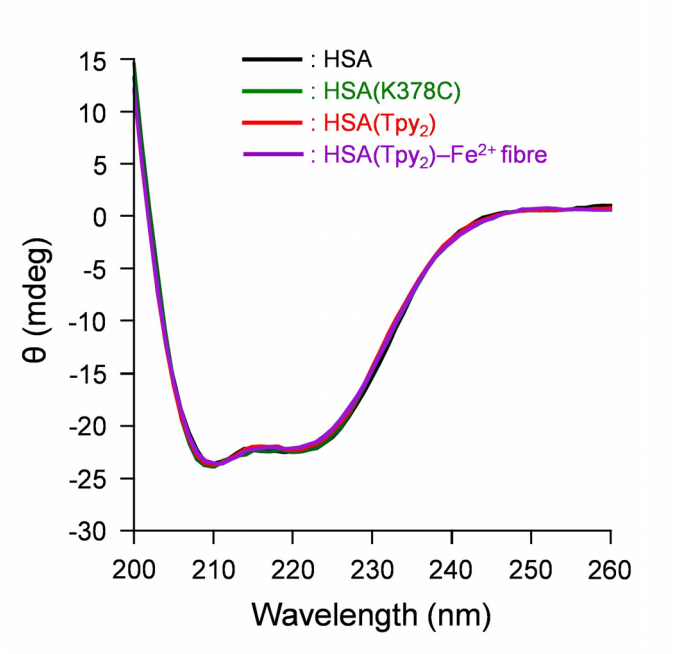


**Fig. S3** CD spectra of HSA($Tpy_2$), HSA(K378C), and HSA, and [HSA($Tpy_2$)–$Fe^{2+}$]$_n$ nanofibres in water at 25°C; [protein] = 10 μM.

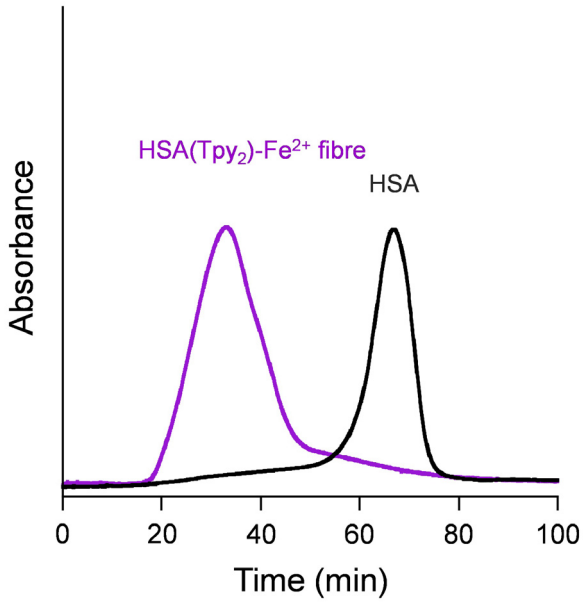


**Fig. S4** SEC elution profiles of [HSA($Tpy_2$)–$Fe^{2+}$]$_n$ nanofibres and HSA in Sephacryl S-300 HR column (GE Healthcare UK Ltd.) at 25°C; eluent: PBS (pH 7.4).

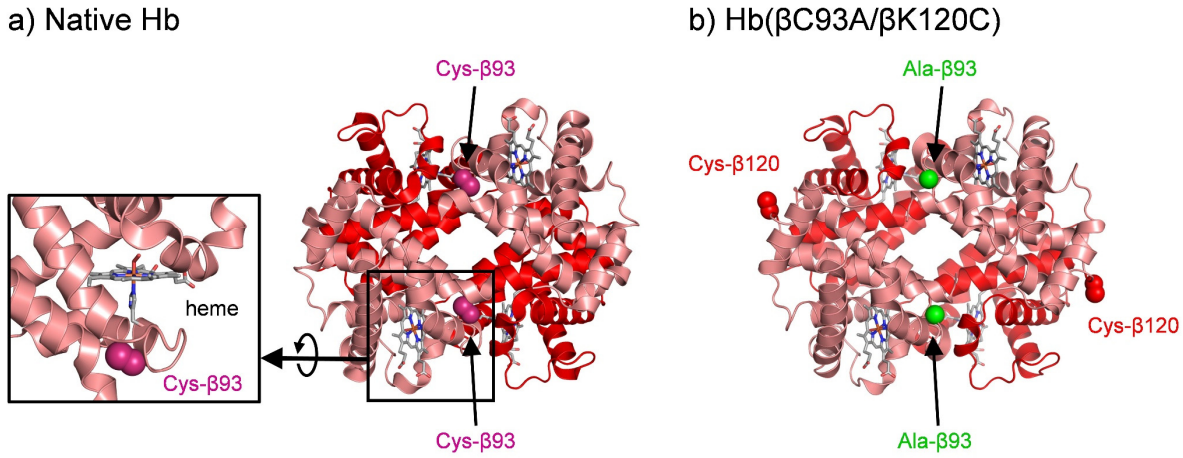


**Fig. S5** Structures of (a) native Hb and (b) Hb(βC93AβK120C) (prepared from PDB ID: 2DN1 from ref. 11).

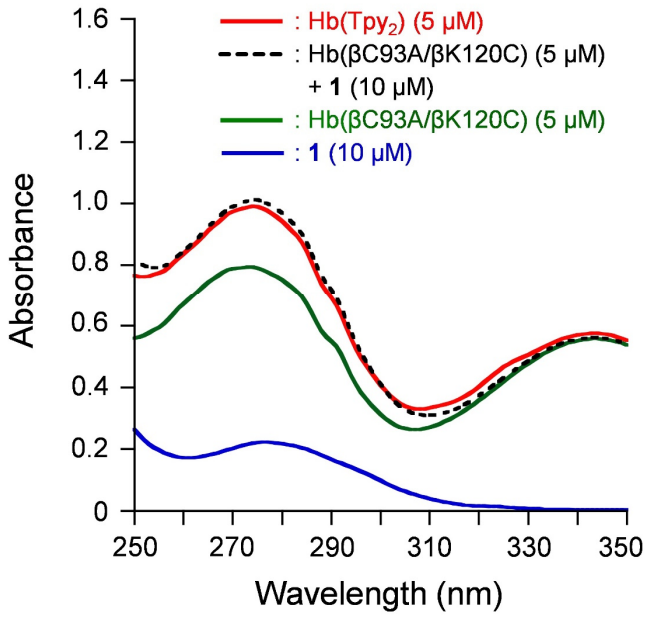


**Fig. S6** UV-vis absorption spectra of Hb($Tpy_2$) in water (5 μM), Hb(βC93A/βK120C) in PB (5 μM), and maleimide-terpyridine (**1**) in DMSO (10 μM) at 25°C.

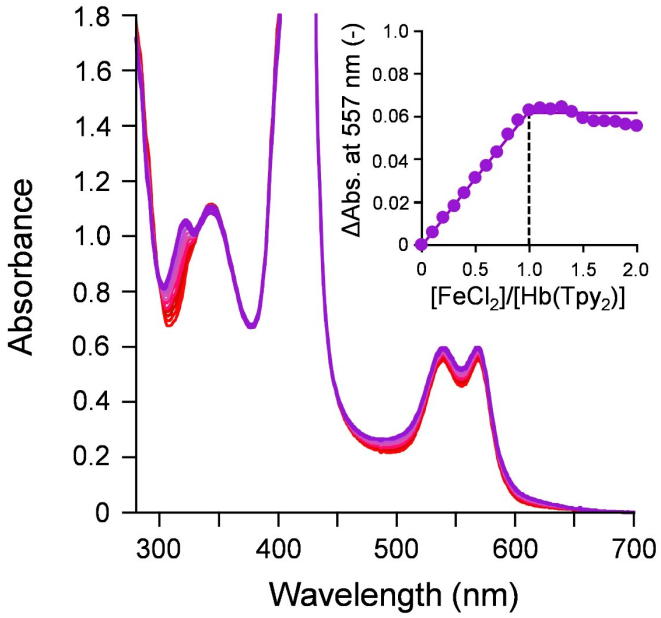


**Fig. S7** UV-vis absorption spectral changes upon addition of $FeCl_2$ into the aqueous $Hb(Tpy_2)$ solution (5.5 μM) at 25°C. (Inset) absorption increase (ΔAbs.) at 557 nm.

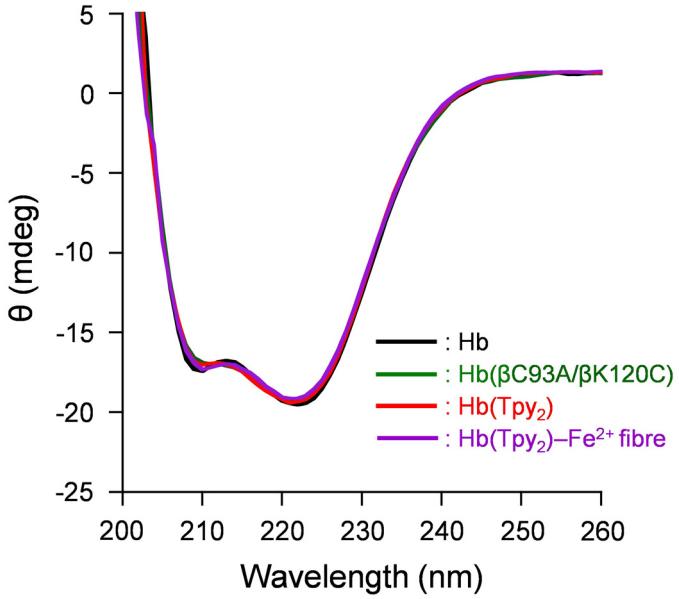


**Fig. S8** CD spectra of $Hb(Tpy_2)$, Hb(βC93A/βK120C), and Hb in PBS (pH 7.4), and $[Hb(Tpy_2)–Fe^{2+}]_n$ nanofibres in water at 25°C; [protein] = 5 μM.

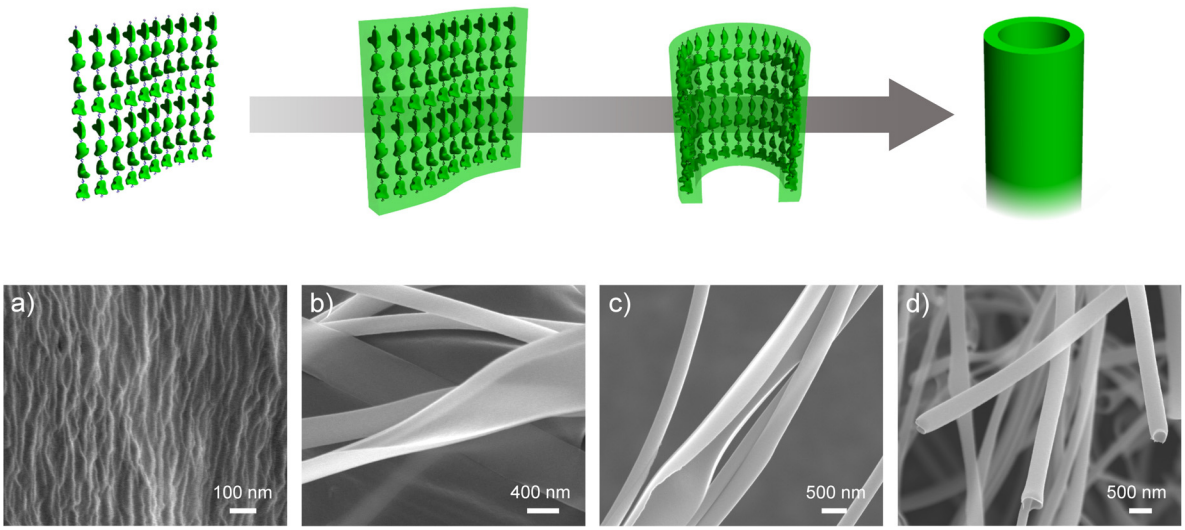


**Fig. S9** SEM images of various forms of [HSA(Tpy$_2$)–Fe$^{2+}$]$_n$ nanotubes prepared by lyophilization. (a) Aligned nanofibres, (b) two-dimensional sheets, (c) open tubules not completely bound, and (d) perfect nanotubes.

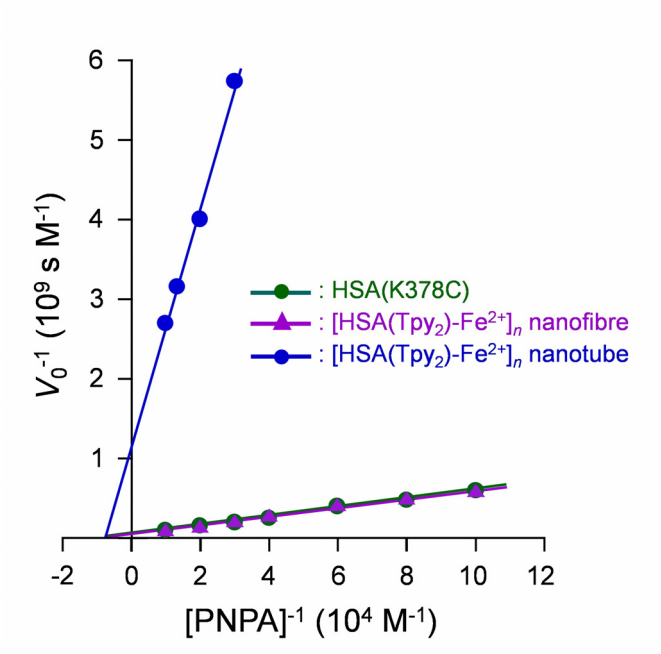


**Fig. S10** Linewever-Burk plots of PNPA hydrolysis using HSA(K378C), [HSA(Tpy$_2$)–Fe$_{2+}$]$_n$ nanofibres, and [HSA(Tpy$_2$)–Fe$_{2+}$]$_n$ nanotubes in PBS (pH 7.4) at 22°C.

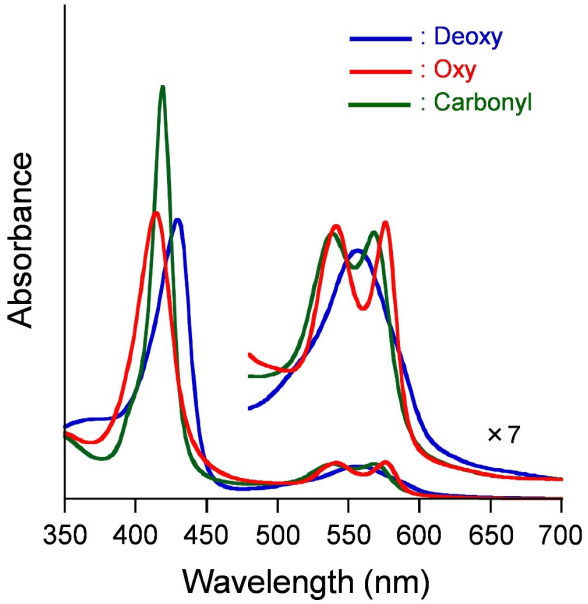


**Fig. S11** UV-vis absorption spectral changes of deoxy, oxy, and carbonyl states of $[Hb(Tpy_2)–Fe_{2+}]_n$ nanofibres in PBS (pH 7.4) at 25°C.

**Table S1.** DLS data of HSA, $HSA(Tpy_2)$, and $[HSA(Tpy_2)–Fe^{2+}]_n$ nanofibres in water (25ºC)

| Proteins | Hydrodynamic diameter (nm) |
|---|---|
| HSA | 6.3 ± 1.9 |
| $HSA(Tpy_2)$ | 7.8 ± 5.8 |
| $[HSA(Tpy_2)–Fe^{2+}]_n$ nanofibre | 160.0 ± 89.9 |

**Table S2.** Visible absorption spectral data of $[Hb(Tpy_2)–Fe^{2+}]_n$ nanofibres in PBS solution (pH 7.4, 25ºC)

| Haemoproteins | $\lambda_{max}$ (nm) | | |
|---|---|---|---|
| | Oxy | Deoxy | Carbonyl |
| Hb | 414, 541, 577 | 430, 555 | 420, 538, 569 |
| Hb(βC93A/βK120C) | 414, 541, 576 | 430, 556 | 419, 538, 569 |
| $[Hb(Tpy_2)–Fe^{2+}]_n$ nanofiber | 414, 542, 576 | 430, 556 | 420, 539, 569 |

**Table S3.** $O_2$ binding parameters of $[Hb(Tpy_2)–Fe^{2+}]_n$ nanofibres in PBS solution (pH 7.4, 37ºC)

| Haemoproteins | $P_{50}$ (Torr) | $n$ (–) |
|---|---|---|
| Hb | 12 | 2.4 |
| Hb(βC93A/βK120C) | 11 | 1.6 |
| $[Hb(Tpy_2)–Fe^{2+}]_n$ nanofibre | 11 | 1.4 |